TNF-α differentially regulates cell cycle genes in promyelocytic and granulocytic HL-60/S4 cells.

Elsie C. Jacobson[1], Lekha Jain[1], Jo K. Perry[1], Mark H. Vickers[1], Ada L. Olins[2], Donald E. Olins[2], Justin M. O'Sullivan[1*]

[1] Liggins Institute, University of Auckland, Auckland, New Zealand
[2]University of New England, Portland, ME, USA

* corresponding author: justin.osullivan@auckland.ac.nz

Author email addresses: ECJ <e.jacobson@auckland.ac.nz>, LJ l.jain@auckland.ac.nz, JKP <j.perry@auckland.ac.nz>, ALO <aolins@une.edu>, DEO <dolins@une.edu>, MHV <m.vickers@auckland.ac.nz>, JMO <justin.osullivan@auckland.ac.nz>

Keywords
Tumor necrosis factor, RNA-seq, differentiation, cell cycle, hematopoiesis, innate immune, neutrophil, macrophage, HL-60, retinoic acid.

Abstract

Tumor necrosis factor alpha (TNF-α) is a potent cytokine involved in systemic inflammation and immune modulation. Signaling responses that involve TNF-α are context dependent and capable of stimulating pathways promoting both cell death and survival. TNF-α treatment has been investigated as part of a combined therapy for acute myeloid leukemia due to its modifying effects on all-trans retinoic acid (ATRA) mediated differentiation into granulocytes.

To investigate the interaction between cellular differentiation and TNF-α, we performed RNA-sequencing on two forms of the human HL-60/S4 promyelocytic leukemia cell line treated with TNF-α. The ATRA-differentiated granulocytic form of HL-60/S4 cells had an enhanced transcriptional response to TNF-α treatment compared to the undifferentiated promyelocytes. The observed TNF-α responses included differential expression of cell cycle gene sets, which were generally upregulated in TNF-α treated promyelocytes, and downregulated in TNF-α treated granulocytes. This is consistent with TNF-α induced cell cycle repression in granulocytes and cell cycle progression in promyelocytes. Moreover, comparisons with gene expression changes associated with differentiation indicated that TNF-α treatment of granulocytes shifts the transcriptome towards that of a macrophage.

We conclude that TNF-α treatment promotes a divergent transcriptional program in promyelocytes and granulocytes. TNF-α promotes cell cycle associated gene expression in promyelocytes. In contrast, TNF-α stimulated granulocytes have reduced cell cycle gene expression, and a macrophage-like transcriptional program.

1. Background

Tumor necrosis factor alpha (TNF-α) is a pro-inflammatory cytotoxic cytokine [1] which activates the innate immune response [2–4], and induces migration [5,6] and production of pro-inflammatory cytokines [7,8]. Dysregulation of TNF-α can be a factor in autoimmune disease [9,10] and anti-TNF antibodies are used to treat a range of inflammatory disorders [11–13]. Initially investigated as a cancer therapeutic due to its ability to promote apoptotic cell death specifically of tumor cells [14], systemic TNF-α treatment has failed clinical trials as a solo cancer therapeutic as it induces unacceptable levels of toxicity [15].

TNF-α signaling is complex with numerous and sometimes conflicting responses being modulated by interaction with two cell surface TNF-α receptors, TNFR1 and TNFR2 [1]. TNF-α binding can have a wide range of effects via activation of signal transduction pathways, including all three groups of mitogen activated kinases (MAPK); extracellular-signal-regulated kinases (ERKs), the cJun NH2-terminal kinases (JNKs), and the p38 MAP kinases [16], which each have complex regulatory effects on the cellular phenotype [17,18]. TNF-α signaling leads to transcriptional upregulation of pro-inflammatory cytokines including *IL-6* [7] and *TNF* itself [8], resulting in pro-inflammatory feedback loops [19]. Notably, TNFR1 and TNFR2 have individual and combinatorial effects on cell death and inflammation [1,20,21]. TNFR1 signaling induces pro-apoptotic pathways resulting in caspase activation, and pro-survival Nuclear Factor Kappa B (NFKB) signaling [22,23]. For example, hematopoietic cells growing in log phase rapidly undergo apoptosis in response to TNF, while quiescent cells in stationary phase re-enter the cell cycle on TNF-α stimulation [24]. These apparently conflicting TNF-α responses can be explained by temporal and developmental effects that include cell type [25], receptor expression [24], priming with cytokines or inflammatory stimuli [26,27], and cell cycle stage [28].

The HL-60/S4 cell line was derived from an acute promyelocytic leukemia patient [29]. These promyelocytic cells can be differentiated into granulocytic or macrophage forms with the addition of all-trans retinoic acid (ATRA) or 12-O-tetradecanoylphorbol-13-acetate (TPA), respectively [30]. Differentiation into the granulocytic form slows cell growth [30] and ultimately leads to cell death [31]. This discovery lead to the clinical use of ATRA as a treatment for acute promyeloid leukemia [32]. Combined treatment with ATRA and TNF-α enhances differentiation of myelogenous leukemia cells, and therefore has been investigated as a synergistic therapy [33,34]. Notably, ATRA-induced differentiation activates components of the TNF-α signaling pathway [33].

A previous study demonstrated differential effects of TNF-α treatment on candidate genes in HL-60 cells before and after ATRA treatment [35]. Here, we investigate the genome-wide transcriptional response to TNF-α treatment of the promyelocytic and granulocytic forms of HL-60/S4 cells. We identify a conserved inflammatory and apoptotic response to TNF-α treatment in both promyelocytic and granulocytic cells. We also identify opposing effects of TNF-α treatment on the expression of cell cycle genes, supporting cell cycle progression in promyelocytes and cell cycle repression in granulocytes. We propose that the different TNF-α mediated responses arise through sets of genes being responsive to different thresholds of total (endogenous and exogenous) TNF-α levels.

2. Results

In order to investigate transcriptional responses to TNF-α, the promyelocytic cell line HL-60/S4 was differentiated into a granulocytic form by treatment with ATRA for 96 hours, as described previously [36]. Both undifferentiated (promyelocytic) and differentiated (granulocytic) cells were treated with 16ng/mL TNF-α in calcium supplemented media for two hours. TNF-α treatment of promyelocytes and granulocytes were run as independent experiments; as a consequence, analysis of transcriptional changes following differentiation was not appropriate. However, a recently published study investigated transcriptional changes following differentiation of promyelocytic HL-60/S4 cells into granulocytes or macrophages [30]. We reanalyzed this data for use in comparisons with the TNF-α response. All genes in both sets of data that were significantly differentially expressed (False discovery rate adjusted p-value (FDR)<0.05) following differentiation or TNF-α treatment were identified (Supp table 1). In order to assess the reproducibility of our data, a subset of differentially expressed genes (*TNF*, *CDK1*, *VCAM1*) were analyzed by RT-qPCR qPCR in a set of independent samples treated as above *i.e.* ± 1 μM ATRA and ± 16ng/mL TNF-α (Supp table 2). Consistent with RNA-seq analysis, RT-qPCR demonstrated that TNF-α stimulated promyelocytes and granulocytes have increased levels of *TNF* and *VCAM1*. *CDK1* increases expression in promyelocytes and decreases expression in granulocytes following TNF-α treatment.

2.1 Gene expression changes after TNF-α treatment of promyelocytic and granulocytic cells

RNA-seq libraries were aligned using an ultrafast universal RNA-seq aligner (STAR [37]) and assigned to genes with featureCounts [38]. DESeq2 [39] was used to filter out lowly-expressed genes and performing differential expression analysis. 14,420 genes were analyzed for TNF-α dependent differential expression in promyelocytes. 21,305 genes were analyzed for TNF-α dependent differential expression in granulocytes. Principal component analysis of variance stabilized transcripts confirmed clustering by treatment (Supp fig 1).

The promyelocytic and granulocytic forms of HL-60/S4 cells both exhibited strong transcriptional responses to TNF-α treatment (Supp table 1). In promyelocytes, 1,312 genes were significantly increased and 980 significantly decreased (FDR adjusted p value < 0.05, Fig 1A). TNF-α treatment of granulocytes significantly increased expression of 3809 genes and decreased expression of 3,597 genes (FDR adjusted p value < 0.05, Fig 1B). Notably, the granulocytic form had more than three times the number of significantly differentially expressed genes (Fig 1C). Despite this, there was significant overlap in the TNF-α dependent transcriptional response between the granulocytic and promyelocytic cells (2.5 fold more than expected by chance, $p<1x10^{-5}$, bootstrapping). The TNF-α treatment consistently resulted in more genes being upregulated than downregulated in both the promyelocytic and granulocytic forms of the HL-60/S4 cells ($p<2x10^{-16}$ and $p=5x10^{-4}$, respectively; 2-sample test for equality of proportions).

Genes that were significantly differentially expressed after TNF-α treatment in both the promyelocytic and granulocytic forms of HL-60/S4 cells exhibited strongly correlated log2 fold changes ($p<2x10^{-16}$, $R^2=0.65$). There was a small subset of differentially expressed genes that exhibited changes in opposite directions in promyelocytes and granulocytes (Fig 1D). Notably, the effect sizes of conserved gene expression changes were similar, with a slope of 1.08. If the observed differences in the numbers of differentially expressed (DE) genes were due to a different magnitude of effect, we would expect to see a correlation in fold change

between genes that were differentially expressed in one cell type but not the other. However, the fold change of non-conserved genes did not strongly correlate between cell types (Fig 1E & F, R^2=0.038, R^2=0.15).

Collectively these results suggest that the difference in TNF-α responses is not simply due to granulocytic cells showing enhanced regulation of a conserved set of genes, resulting in a greater number that are significantly differentially expressed. Instead, additional sets of genes are changing transcriptional activity in TNF-α treated granulocytes.

2.2 Functional analysis of the TNF-α response in promyelocytes and granulocytes

Functional analysis of gene sets is affected by the available gene function information, and the method of enrichment analysis [40]. Therefore, we used multiple annotation sources (*i.e.* Molecular Signatures Databaste (MSigDB) hallmark gene sets [41], gene ontology (GO) [42], and Kyoto Encyclopedia of Genes and Genomes (KEGG) pathways [43]) to interrogate the TNF-α response in HL-60/S4 cells and identify robust enrichment results.

2.2.1 Gene set enrichment analysis of promyelocytes and granulocytes treated with TNF

We first interrogated the global gene expression changes that occurred in the two different cell types after TNF-α treatment. Gene set enrichment analysis (GSEA) is a method that allows analysis of an entire differential expression dataset without using arbitrary significance thresholds [44]. Instead, the entire dataset is ranked by log2 fold change, and terms are considered enriched if they are overrepresented at the top or bottom of the ranked list. This approach allows for a differentiation between functional categories of genes that are upregulated or downregulated after treatment [45], and provides an overview of transcriptional changes.

We performed GSEA of hallmark gene sets (Supp table 3). We found a strong upregulation response to TNF-α, in both the promyelocytic and granulocytic forms of the HL-60/S4 cells, that was characterized by immune and cell death pathways (Fig 2). However, the granulocytic genes that were upregulated were also enriched for terms that included notch signaling and hypoxia. Transcripts associated with WNT and beta-catenin signaling were downregulated in promyelocytes (Fig 2).

As observed in the differentially expressed genes, GSEA showed a strong conserved response with notable divergences between TNF-α stimulated promyelocytes and granulocytes.

2.2.2 Functional analysis of conserved, cell type-specific, and opposite TNF-α responses

In order to further investigate the similarities and differences in the TNF-α response, we grouped the list of analyzed genes based on the direction and significance of the expression change in each cell type. Genes that were differentially expressed following TNF-α treatment were divided into four groups according to the nature of the correlation between the promyelocytic and granulocytic responses: 1) conserved; 2) promyelocyte-specific; 3) granulocyte-specific; and 3) opposite responses (Supp table 1). The first group represents the conserved response, *i.e.* the genes were significantly differentially expressed in the same direction in both promyelocytic and granulocytic forms of the HL-60/S4 cells. The next two groups represent cell type-specific responses – *i.e.* genes that were only differentially

expressed in either promyelocytes or granulocytes in response to TNF-α treatment. The final group is comprised of the 157 genes that were significantly upregulated in the first cell type and significantly downregulated in the other cell type, or *vice versa*.

Having identified groups of genes that change in a conserved, cell-type specific, and opposite manner, we performed functional enrichment analyses to further investigate the responses to TNF-α in promyelocytes and granulocytes.

2.2.2.1 A conserved TNF-α response

Genes that exhibited significant changes in the same direction in response to TNF-α treatment in both promyelocytic and granulocytic forms of the HL-60/S4 cells were more frequently upregulated than downregulated (~3:1). Notably, this trend was not maintained for cell type-specific gene expression changes (promyelocyte-specific ~1.2:1, granulocyte-specific ~0.9:1). There were nine enriched MSigDB hallmark gene sets [41] in the conserved response gene set (Fig 3A, Supp table 4), all of which are associated with well described effects of TNF-α stimulation; cytokine signaling, inflammation, and apoptosis. This was broadly consistent with the results of GSEA (Fig 2). The top three enriched pathways within KEGG were: NFKB Signaling; NOD-like receptor signaling; and TNF-α signaling pathways (Supp table 5). The top 10 enriched GO terms included interferon-gamma (IFNγ)-mediated signaling pathway, inflammatory response, and positive regulation of I-kappaB kinase/NFKB signaling (Supp table 6).

In summary, using three different annotation databases and four different analysis approaches, we have shown that TNF-α treatment of both promyelocytic and granulocytic forms of HL-60/S4 cells induces a transcription profile associated with inflammatory responses and NFKB signaling.

2.2.2.2 Granulocyte-specific TNF-α responses

The cell type-specific promyelocytic DE genes had no significant enrichments of MSigDB gene sets, KEGG pathways, or GO terms. Cell type-specific granulocytic DE genes were enriched for MSigDB sets related to cell cycle and energetics (Fig 3B, Supp table 7). The top five enriched KEGG pathways included Cell Cycle, Protein processing in endoplasmic reticulum, and Cellular senescence (Supp table 8). The six enriched GO terms included cell division, G2/M transition of mitotic cell cycle, protein poly- and de-ubiquitination, and neutrophil degranulation (Supp table 9). Thus, granulocytes, but not promyelocytes, exhibited transcriptional changes in genes involved in cell cycle and protein processing in response to TNF-α treatment.

2.2.2.3 Opposite TNF-α responses in promyelocytes and granulocytes

Genes that were significantly differentially expressed in opposite directions in promyelocytes and granulocytes were enriched for G2M checkpoint and E2F targets within the MSigDB database (Fig 3C, Supp table 10). Differentially expressed genes in these sets were upregulated in promyelocytes and downregulated in granulocytes, with the exception of *E2F2*. *CDK1* is included in both of these cell-cycle associated gene sets, and is considered sufficient to drive the mammalian cell cycle [46]. As described above, the upregulation and downregulation of *CDK1* in promyelocytes and granulocytes respectively was confirmed by

RT-qPCR (Supp table 2). The set of genes that was significantly expressed in opposite directions was also enriched for three terms, including mitotic chromosome condensation, within the GO database (Supp table 11). There was no enrichment for pathways within KEGG.

The inflammatory effects of TNF-α stimulation are shared by promyelocytes, but cell cycle repression and altered protein metabolism are TNF-α responses specific to granulocytes.

2.3 Granulocytic differentiation increases transcript levels of TNF and TNF receptors

We set out to investigate how differentiation into the granulocytic form could modulate the TNF-α response, and identify similarities in the transcriptional changes that occur during differentiation and acute TNF-α treatment. We were unable to analyze transcriptional changes that occurred during differentiation, as promyelocytic and granulocytic cells were treated with TNF-α in separate experiments. In order to assess gene expression changes associated with differentiation we analyzed publicly available RNA-seq data of HL-60/S4 cells differentiated into granulocytes (with ATRA) and macrophages (with TPA). Principal component analysis of variance stabilized transcripts confirmed clustering by differentiation status (Supp fig 1C).

Consistent with previous reports [30], this analysis confirmed that *TNF* expression was upregulated during differentiation into either granulocytic or macrophage forms of HL-60/S4 cells. The magnitude of *TNF* transcript upregulation was different in granulocytes ($\log_2$ fold change = 1.37) and macrophages ($\log_2$ fold change = 4.08) (Supp table 1). Differentiation also induced changes in the expression levels of the TNFRs. Consistent with previous observations [30], *TNFRSF1A* gene expression was increased ($\log_2$ fold change = 0.87) after ATRA treatment, but there was no significant change in expression following TPA treatment. By contrast, *TNFRSF1B* gene expression was increased in both conditions ($\log_2$ = 1.59 and 3.30 following ATRA and TPA treatment, respectively). This observed increase in mRNA expression of *TNF* and both TNF-α receptors may be one explanation for why granulocytes have an enhanced transcriptional response to TNF-α, compared to promyelocytes.

We investigated whether TNF-associated genes were enriched for transcriptional changes associated with differentiation into the granulocytic or macrophage form. We performed a GSEA of the transcriptional changes associated with differentiation into the granulocytic and macrophage form (Fig 4). As described previously, genes associated with cell-cycle terms (e.g. MYC targets and G2M checkpoint) were downregulated, while genes associated with inflammatory terms (e.g. IFNγ response, inflammatory response, and indeed TNF-α signaling via NFKB) were upregulated in both differentiation experiments (Fig 4).

As shown in Welch *et. al.* [30], differentiation into either the granulocytic or macrophage form resulted in higher inflammatory gene expression and lower cell cycle rate.

2.4 TNF-α treatment has more shared responses with TPA treatment than ATRA treatment

TNF-α treatment interacts with ATRA to augment differentiation of myeloid cells [33,34], but whether it enhances the differentiation into granulocytic cells or modifies the differentiation trajectory is unclear. We compared the transcriptional changes of TNF-α

treated granulocytes with those associated with differentiation into granulocytes or macrophages.

Gene sets upregulated in TNF-α stimulated granulocytes and differentiated granulocytes or macrophages were enriched for ontological terms associated with hypoxia and xenobiotic metabolism. Notably, genes that were upregulated in promyelocytes treated with TNF-α did not show enrichment for these ontological terms. Notch signaling was upregulated only after TNF-treatment of promyelocytes or differentiation into macrophages. Intriguingly, both early and late estrogen response genes were upregulated in granulocytes treated with TNF-α, and macrophages, despite reports that TNF-α acts to oppose estrogen signaling in breast cancer [47]. Four terms were upregulated after TNF-α treatment of granulocytes and differentiation into macrophages: IL2 stat5 signaling, epithelial mesenchymal transition, apical junction, and KRAS signaling (genes downregulated by KRAS activation) (Fig 4).

To further compare the transcriptional changes that occur during differentiation into different cell types with the effects of TNF-α treatment, we assigned differentiation associated changes into four groups: 1) conserved; 2) granulocyte-specific; 3) macrophage-specific; and 4) opposite, *i.e.* significantly upregulated in granulocytes and significantly downregulated in macrophages, or vice versa (Supp table 1). The first group consists of genes that significantly change expression levels in the same direction after differentiation into either the granulocytic from with ATRA, or the macrophage form with TPA. The second and third groups contain genes that are differentially expressed only after differentiation into granulocytes or macrophages, but not both. The fourth group represents genes that are differentially expressed after differentiation into granulocytes and macrophages, but are upregulated in granulocytes and downregulated in macrophages, or vice versa. We analyzed these groups of genes for enrichment of MSigDB gene sets, KEGG pathways, and GO terms. GSEA identified the response that is conserved during differentiation into granulocytes or macrophages as being characterized by pro-inflammatory cytokine associated gene sets (*i.e.* IFNα, response, IFNγ response, TNF-α signaling via NFKB), and cell cycle associated gene sets (*i.e.* G2M checkpoint, MYC targets, and mitotic spindle) (Fig 5A). This finding was consistent with what was observed as being enriched within the KEGG pathways and GO terms (Supp table 13,14).

Genes that changed expression after differentiation into granulocytes, but not macrophages, were not enriched for MSigDB gene sets or GO terms, but they were enriched for three KEGG pathways related to protein processing (Protein processing in endoplasmic reticulum, ubiquitin mediated proteolysis, and proteasome; Supp table 15). In contrast, genes that changed expression after differentiation into macrophages, but not granulocytes, were enriched for several MSigDB gene sets related to cell cycle (Fig 5B, Supp table 16). Enriched KEGG pathways included metabolism and protein processing (*i.e.* carbon metabolism and protein processing in endoplasmic reticulum), and the TNF-α signaling pathway (Supp table 17). Enriched GO terms included cell division, and terms related to RNA and protein regulation (*i.e.* regulation of transcription, DNA-templated, translational initiation).

2.4.1 Convergence of transcriptional programs in macrophages and TNF-treated granulocytes

There are many similarities between the behaviors of HL-60/S4 cells differentiated into granulocytes and macrophages. However, there are also notable behavioral differences that

include macrophages exhibiting a decreased cell cycle rate, increased survival, and adhesion to both surfaces and other cells [30].

We investigated the genes that were significantly differentially expressed with negatively correlated log2 fold changes after differentiation into granulocytes or macrophages – *i.e.* in opposite directions. This gene set was enriched for the IL2/STAT5 signaling, p53 pathway, and TNF-α signaling MSigDB hallmark terms (Fig 5C). 91% of these genes (102/112) increased expression after macrophage differentiation, and decreased expression after granulocytic differentiation. 65% of these genes (70/112) significantly increased expression in granulocytes treated with TNF-α, while only 10% (12/112) significantly decreased expression (Fig 5C). Six transcription factors (*ATF3*, *BCL6*, *FOSL1*, *KLF4*, *KLF9*, *NR4A1*) increased expression after macrophage differentiation and granulocytes treated with TNF-α, but decreased expression after granulocytic differentiation, which indicates a shared change in transcriptional programming. *CD83*, which is a marker of transdifferentiation of neutrophils into a dendritic-type cell, increased in both TNF-α treated cell types [48,49]. Given that macrophages and dendritic cells are phenotypically similar [50,51], *CD83* could be considered a marker of macrophage transdifferentiation.

Collectively our analyses suggest that TNF-α alters the transcriptional profile in HL-60/S4 cells consistent with a transition from a granulocytic to macrophage phenotype. Consistent with previous observations [33,34], TNF-α modifies the differentiation trajectory away from the ATRA induced granulocytic phenotype, towards a macrophage-like phenotype.

Discussion

TNF-α treatment causes dramatic changes in the transcriptional programs of both promyelocytic and granulocytic HL-60/S4 cells. In this study we found that ATRA and TPA directed differentiation or TNF-α treatment of differentiated HL-60/S4 cells resulted in canonical TNF-α responses involving NKFB signaling, inflammatory signaling, p53 and apoptosis. Due to the reduced proliferation of granulocytic HL-60/S4 cells [30] we expected differential cell cycle effects of TNF-α treatment [24,28]. Previous work has shown increased proliferation in quiescent cells, while proliferating cells exhibited increased apoptosis after TNF-α treatment [24]. In contrast, we saw evidence of cell cycle repression in granulocytes, particularly at mitotic entry, while proliferating promyelocytes had an increase in cell cycle progression markers such as *CDK1* [46].

There are several factors that could explain the different responses of promyelocytes and granulocytes to TNF-α. Firstly, granulocytes have increased levels of endogenous TNF-α production. Not only does this increase the total TNF-α the cells are exposed to, but endogenously produced TNF-α is membrane-bound prior to processing [52]. The transmembrane and soluble forms of TNF-α have different effects [53], possibly due to the activation of different TNFRs. Membrane-bound TNF-α can activate both TNFR1 (*TNFRSF1A*) and TNFR2 (*TNFRSF1B*), but soluble TNF-α can only activate TNFR1 [54]. Granulocytic cells have higher levels of endogenous *TNF* expression (therefore, likely higher levels of transmembrane TNF-α) and concurrently higher levels of both *TNFRSF1A* and *TNFRSF1B* gene expression [55]. It has been previously proposed that increased levels of TNFR2 in granulocytic HL-60 cells explain their resistance to TNF-α induced apoptosis [35]. Thus, it may be not just the increased levels of receptors, but the ratio of TNFR1 to TNFR2 that determines the ultimate response to TNF-α.

The TNFR1 and TNFR2 receptors have uniquely stimulated pathways [56,57], however the two receptors also interact to produce a context specific TNF-α response [58,59]. Therefore, manipulating exogenous and endogenous levels of TNF-α or changing the ratio of the TNFR1 and TNFR2 receptors will provide greater insight into the phenotypic consequences of TNF-α treatment. Based on our data, we predict a dose dependent effect of total TNF-α on gene expression, whereby a low level of TNF-α is sufficient to induce regulation of the set of genes seen in the promyelocyte response, while higher levels of TNF-α are required to repress cell cycle. However, cell cycle repression likely also requires the presence of additional factors (*e.g.* TNFR-associated factors [60]) that are expressed during differentiation of the HL-60/S4 cells into the granulocytic form.

A reduction in the expression of cell cycle genes at the population level indicates a change in the proportion of cells at different stages of the cell cycle. Due to the massive transcriptional changes that occur during the progression through cell cycle [61–64], this may obscure other gene regulatory programs that are associated with alterations to cell function. Despite this limitation, we found evidence of a subset of TNF-α-regulated genes that were upregulated in TNF-treated granulocytes and following macrophage differentiation, but downregulated after granulocytic differentiation. These genes encoded a suite of transcription factors, and the dendritic cell surface marker CD83. Neutrophils that take on characteristics of antigen-presenting cells are often characterized by increased levels of CD83 [48,49], suggesting that TNF-α may be stimulating transdifferentiation. This is not unprecedented, as there is evidence that neutrophils have phenotypic plasticity [65], and that TNF-α can stimulate transdifferentiation [66–68]. However, further functional characterization of TNF-α-treated granulocytic HL-60/S4 cells is required to confirm this hypothesis.

A large-scale TNF-α response experiment treating many different cell types at various stages of differentiation would allow a network analysis of the transcriptional responses and annotation-free pathway discovery [69,70]. This would provide data to test our hypothesis that total TNF-α exposure correlates with repressive effects on the cell cycle. If this experiment were performed with single cell RNA-sequencing it would also enable the investigation of how individual TNF-α responses result in population-wide changes in cell cycle gene expression. For instance, do all cells respond to TNF-α stimulation with cytokine production, G2/M arrest, and apoptosis, or is there a heterogeneous response between different cells in a population? Moreover, single cell data would allow us to adjust for the cell cycle transcriptional effects, and identify differences that were previously masked by the population structure of unsynchronized cells.

Despite being one of the most highly studied genes in the human genome [71], the complex signaling [1] and context dependent effects [20,28,56] of TNF-α mean that much of its biology remains unknown. With the increasing accessibility of modern sequencing technologies and gene editing, high-throughput investigations of the TNF-α response and signaling will yield new results that enable the contextualization of TNF-α in cancer and immunology.

Conclusion

HL-60/S4 cells show a conserved set of core responses to TNF-α treatment irrespective of the differentiation state of the cell. This is expected, since functional annotations represent

canonical pathways and responses. However, granulocytes are more responsive to TNF-α, possibly due to priming from increased endogenous *TNF* expression, and increased levels of TNF-α receptors. Transcriptional changes indicate that TNF-α treatment represses cell cycle progression in granulocytes, but has the opposite effect on promyelocytes. This effect may be sensitive to the sum total of the exogenous and endogenous TNF-α levels. Finally, comparisons of transcriptional changes during differentiation and TNF-α treatment suggest that TNF-α treatment of granulocytes pushes them towards a macrophage transcriptional program. The context specific effects of TNF-α are likely mirrored in other models of innate immune signaling, and may contribute to the disparities seen between *in vitro* and *in vivo* studies of innate immune signaling.

Methods

Cell culture

HL-60/S4 cells (available from ATCC #CCL-3306) were cultured at 37°C, 5% CO_2 in RPMI 1640 (ThermoFisher) supplemented with 10% fetal bovine serum (Moregate Biotech), 1% penicillin/streptomycin (ThermoFisher), 1% GlutaMAXTM (ThermoFisher) and 2mM $CaCl_2$.

As required, cells were differentiated into a granulocytic phenotype with 1 µM all trans retinoic acid (ATRA) dissolved in ethanol (Sigma Aldrich) for four days as previously described ([30,36,72]). Cells were centrifuged (200xg, 5 min, room temp.) and suspended (undifferentiated = $1x10^6$ cells/mL; or differentiated = $5x10^5$ cells/mL) in fresh media (with 1µM ATRA for differentiated cells). Nuclear morphology and cell surface receptor changes during differentiation are available from Jacobson *et. al.* 2018 [36]. Hi-C and RNA-seq were used to identify translocations and other structural variants specific to HL-60/S4 [73]. Cells from the same seed-lot were used in all studies.

Cells (9 x 10^6 per flask) were incubated at 37ºC for 2 hours before addition of 16ng/mL TNF-α or vehicle in triplicate per condition. After 2 hours treatment, cells in each flask were lysed with TRIzol LS (Life Technologies), phase separated with chloroform, and RNA extracted with the Qiagen RNeasy mini kit (Qiagen, 74104). A summary of the conditions in this study, and the public data from Welch 2017 [30], are shown in table 1.

The full experiment was repeated and samples analyzed with RT-qPCR of *TNF*, *CDK1*, and *VCAM1* to validate the RNA-seq results (see below).

RNA sequencing

Total RNA libraries were prepared by Annoroad Gene Technology Co., Ltd. (Beijing, China) using ribosomal RNA depletion with RiboZero Magnetic Gold Kit (Human/Mouse/Rat) and sequenced on an Illumina Hi-seq X 150PE (150 base pair paired end reads).

Publicly available RNA-seq

mRNA-seq data of HL-60/S4 cells in three conditions in quadruplet [30] was downloaded from NCBI (http://www.ncbi.nlm.nih.gov/bioproject/303179). These conditions are: HL-60/S4 (promyelocytes), HL-60/S4 differentiated with ATRA (granulocytes), and HL-60/S4 differentiated with TPA (macrophage-like).

RNA-seq analysis

Read quality was confirmed using FastQC v0.11.4. Paired end reads were aligned to hg38 and gencode annotations v27 using STAR [37] v2.5.3a with default settings. FeatureCounts [38] v1.5.2 was used to aggregate transcripts for gene-level analysis and quantify the reads with GENCODE [74] annotations v27. MultiQC [75] was used to summarize FastQC, STAR, and FeatureCounts outputs [75]. Mapping statistics are summarized in table 1.

Expressed genes were filtered (default settings) and differentially expressed genes (FDR<0.05) identified in DEseq2 [39] v1.16.1. Gene ontology enrichments were calculated with TopGo [42] v2.28.0 using the weight01 algorithm and the Fisher statistic. Categories containing <2 genes were removed, and p values adjusted for FDR. Kegg pathway analysis, GSEA, and enrichment analyses were performed using clusterProfiler [76]. Intersects were displayed with Vennerable [77], subsets extracted with dplyr [78], and plots were generated with ggplot2 [79] in R.

RNA-seq data was also used to check for mycoplasma contamination, as performed in [80]. All libraries were aligned to the genomes of four common mycoplasma species known to contaminate mammalian cell culture: *Mycoplasma hominis* ATCC 23114 (NC_013511.1), *M. hyorhinis* MCLD (NC_017519.1), *Mycoplasma fermentans* M64 (NC_014921.1) and *Acholeplasma laidlawii* PG-8A (NC_010163.1). The fasta genome sequences and genome annotation files were downloaded from NCBI Genome, and genome indices were created with STAR 2.6.0c. Due to their small genome size, the parameter genomeSAindexNbases was adjusted for each genome to the recommended log2(GenomeLength)/2 – 1. Zero reads from any of the 12 libraries aligned to any of the four mycoplasma genomes, confirming that our cultures were free from mycoplasma contamination.

Quantitative real-time PCR

Total RNA was isolated using Trizol LS (Life Technologies). RNA was quantified using a NanoDrop spectrophotometer (NanoDrop Technologies). Isolated RNA was deoxyribonuclease I treated (Life Technologies). Single-stranded cDNA was synthesized from 1 µg of RNA using a High capacity cDNA RT kit (Thermofisher # 4368814), according to the manufacturer's protocol. Real-time quantitative PCR analysis was carried out using predesigned PrimeTime® Mini qPCR assays (Integrated DNA Technologies; Supp table 22) on a Lightcycler 480 (Roche). mRNA levels were normalized using reference genes (*GAPDH* and *COX4I1*). Log2 fold changes and errors was calculated using R using the delta-delta Ct method [81].

Data availability

TNF-alpha treatment RNA-seq data is available on GEO, accession GSE120579. Differentiation RNA-seq data from [30] is publicly available on NCBI, http://www.ncbi.nlm.nih.gov/bioproject/303179. Analysis of processed RNA-seq data is available on github, https://github.com/jacel/TNF_HL60_S4.

References

1 Sedger LM, McDermott MF. TNF and TNF-receptors: From mediators of cell death

and inflammation to therapeutic giants – past, present and future. Cytokine Growth Factor Rev 2014;25:453–472.
2 Mizgerd JP, Spieker MR, Doerschuk CM. Early response cytokines and innate immunity: essential roles for TNF receptor 1 and type I IL-1 receptor during Escherichia coli pneumonia in mice. J Immunol 2001;166:4042–4048.
3 Francisco NM, Hsu N-J, Keeton R, et al. TNF-dependent regulation and activation of innate immune cells are essential for host protection against cerebral tuberculosis. J Neuroinflammation 2015;12:125.
4 Striz I, Brabcova E, Kolesar L, et al. Cytokine networking of innate immunity cells: a potential target of therapy. Clin Sci 2014;126:593–612.
5 Vieira SM, Lemos HP, Grespan R, et al. A crucial role for TNF-alpha in mediating neutrophil influx induced by endogenously generated or exogenous chemokines, KC/CXCL1 and LIX/CXCL5. Br J Pharmacol 2009;158:779–789.
6 Smart SJ, Casale TB. TNF-alpha-induced transendothelial neutrophil migration is IL-8 dependent. Am J Physiol 1994;266:L238-45.
7 Shalaby MR, Waage A, Aarden L, et al. Endotoxin, tumor necrosis factor-alpha and interleukin 1 induce interleukin 6 production in vivo. Clin Immunol Immunopathol 1989;53:488–498.
8 Kagoya Y, Yoshimi A, Kataoka K, et al. Positive feedback between NF-κB and TNF-α promotes leukemia-initiating cell capacity. J Clin Invest 2014;124:528–542.
9 Chu CQ, Field M, Feldmann M, et al. Localization of Tumor Necrosis Factor α in synovial tissues and at the Cartilage–Pannus Junction in patients with rheumatoid arthritis. Arthritis Rheum 1991;34:1125–1132.
10 Palucka AK, Blanck J-P, Bennett L, et al. Cross-regulation of TNF and IFN-alpha in autoimmune diseases. Proc Natl Acad Sci 2005;102:3372–3377.
11 Maxwell LJ, Zochling J, Boonen A, et al. TNF-alpha inhibitors for ankylosing spondylitis. Cochrane Database Syst Rev 2015.
12 Feldmann M. Development of anti-TNF therapy for rheumatoid arthritis. Nat Rev Immunol 2002;2:364–371.
13 Chowers Y, Allez M. Efficacy of anti-TNF in Crohn's disease: how does it work? Curr Drug Targets 2010;11:138–142.
14 Ziegler-Heitbrock HW, Möller A, Linke RP, et al. Tumor necrosis factor as effector molecule in monocyte mediated cytotoxicity. Cancer Res 1986;46:5947–5952.
15 Roberts NJ, Zhou S, Diaz LA, et al. Systemic use of tumor necrosis factor alpha as an anticancer agent. Oncotarget 2011;2:739–751.
16 Sabio G, Davis RJ. TNF and MAP kinase signalling pathways. Semin Immunol 2014;26:237–245.
17 Plotnikov A, Zehorai E, Procaccia S, et al. The MAPK cascades: Signaling components, nuclear roles and mechanisms of nuclear translocation. Biochim Biophys Acta - Mol Cell Res 2011;1813:1619–1633.
18 Kim EK, Choi E-J. Pathological roles of MAPK signaling pathways in human diseases. Biochim Biophys Acta - Mol Basis Dis 2010;1802:396–405.
19 Yarilina A, Park-Min K-H, Antoniv T, et al. TNF activates an IRF1-dependent autocrine loop leading to sustained expression of chemokines and STAT1-dependent type I interferon–response genes. Nat Immunol 2008;9:378–387.
20 Rauert H, Stühmer T, Bargou R, et al. TNFR1 and TNFR2 regulate the extrinsic apoptotic pathway in myeloma cells by multiple mechanisms. Cell Death Dis 2011;2:e194–e194.
21 Kalb A, Bluethmann H, Moore MW, et al. Tumor necrosis factor receptors (Tnfr) in mouse fibroblasts deficient in Tnfr1 or Tnfr2 are signaling competent and activate the

mitogen-activated protein kinase pathway with differential kinetics. J Biol Chem 1996;271:28097–28104.
22 Ting AT, Bertrand MJM. More to life than NF-κB in TNFR1 signaling. Trends Immunol 2016;37:535–545.
23 Annibaldi A, Meier P. Checkpoints in TNF-induced cell death: implications in inflammation and cancer. Trends Mol Med 2018;24:49–65.
24 Baxter GT, Kuo RC, Jupp OJ, et al. Tumor necrosis factor-alpha mediates both apoptotic cell death and cell proliferation in a human hematopoietic cell line dependent on mitotic activity and receptor subtype expression. J Biol Chem 1999;274:9539–9547.
25 Ajibade AA, Wang HY, Wang R-F. Cell type-specific function of TAK1 in innate immune signaling. Trends Immunol 2013;34:307–316.
26 Wang F, Schwarz BT, Graham WV, et al. IFN-γ-induced TNFR2 expression is required for TNF-dependent intestinal epithelial barrier dysfunction. Gastroenterology 2006;131:1153–1163.
27 Erwig LP, Kluth DC, Walsh GM, et al. Initial cytokine exposure determines function of macrophages and renders them unresponsive to other cytokines. J Immunol 1998;161:1983–1988.
28 Darzynkiewicz Z, Williamson B, Carswell EA, et al. Cell cycle-specific effects of tumor necrosis factor. Cancer Res 1984;44:83–90.
29 Gallagher R, Collins S, Trujillo J, et al. Characterization of the continuous, differentiating myeloid cell line (HL-60) from a patient with acute promyelocytic leukemia. Blood 1979;54:713–733.
30 Mark Welch DB, Jauch A, Langowski J, et al. Transcriptomes reflect the phenotypes of undifferentiated, granulocyte and macrophage forms of HL-60/S4 cells. Nucleus 2017;8:222–237.
31 Ozeki M, Shively JE. Differential cell fates induced by all-trans retinoic acid-treated HL-60 human leukemia cells. J Leukoc Biol 2008;84:769–779.
32 Su M, Alonso S, Jones JW, et al. All-trans retinoic acid activity in acute myeloid leukemia: Role of cytochrome P450 enzyme expression by the microenvironment. PLoS One 2015;10:e0127790.
33 Witcher M, Ross DT, Rousseau C, et al. Synergy between all-trans retinoic acid and tumor necrosis factor pathways in acute leukemia cells. Blood 2003;102.
34 Bruserud Ø. New strategies for the treatment of acute myelogenous leukemia: Differentiation induction - present use and future possibilities. Stem Cells 2000;18:157–165.
35 Vondrácek J, Sheard MA, Krejcí P, et al. Modulation of death receptor-mediated apoptosis in differentiating human myeloid leukemia HL-60 cells. J Leukoc Biol 2001;69:794–802.
36 Jacobson EC, Perry JK, Long DS, et al. Migration through a small pore disrupts inactive chromatin organization in neutrophil-like cells. BMC Biol 2018;16:142.
37 Dobin A, Davis CA, Schlesinger F, et al. STAR: ultrafast universal RNA-seq aligner. Bioinformatics 2013;29:15–21.
38 Liao Y, Smyth GK, Shi W. featureCounts: an efficient general purpose program for assigning sequence reads to genomic features. Bioinformatics 2014;30:923–930.
39 Love MI, Huber W, Anders S. Moderated estimation of fold change and dispersion for RNA-seq data with DESeq2. Genome Biol 2014;15:550.
40 Huang DW, Sherman BT, Lempicki RA. Bioinformatics enrichment tools: paths toward the comprehensive functional analysis of large gene lists. Nucleic Acids Res 2009;37:1–13.

41 Liberzon A, Birger C, Thorvaldsdóttir H, et al. The molecular signatures database hallmark gene set collection. Cell Syst 2015;1:417–425.
42 Alexa A, Rahnenfuhrer J. topGO: Enrichment analysis for gene ontology 2016.
43 Ogata H, Goto S, Sato K, et al. KEGG: Kyoto encyclopedia of genes and genomes. Nucleic Acids Res 1999;27:29–34.
44 Subramanian A, Tamayo P, Mootha VK, et al. Gene set enrichment analysis: A knowledge-based approach for interpreting genome-wide expression profiles. Proc Natl Acad Sci 2005;102:15545–15550.
45 Mootha VK, Lindgren CM, Eriksson K-F, et al. PGC-1α-responsive genes involved in oxidative phosphorylation are coordinately downregulated in human diabetes. Nat Genet 2003;34:267–273.
46 Santamaría D, Barrière C, Cerqueira A, et al. Cdk1 is sufficient to drive the mammalian cell cycle. Nature 2007;448:811–815.
47 Lee S-H, Nam H-S. TNF alpha-induced down-regulation of estrogen receptor alpha in MCF-7 breast cancer cells. Mol Cells 2008;26:285–290.
48 Iking-Konert C, Csekö C, Wagner C, et al. Transdifferentiation of polymorphonuclear neutrophils: acquisition of CD83 and other functional characteristics of dendritic cells. J Mol Med (Berl) 2001;79:464–474.
49 Iking-Konert C, Wagner C, Denefleh B, et al. Up-regulation of the dendritic cell marker CD83 on polymorphonuclear neutrophils (PMN): divergent expression in acute bacterial infections and chronic inflammatory disease. Clin Exp Immunol 2002;130:501–508.
50 Hume DA. Macrophages as APC and the dendritic cell myth. J Immunol 2008;181:5829–5835.
51 Hashimoto D, Miller J, Merad M. Dendritic cell and macrophage heterogeneity in vivo. Immunity 2011;35:323–335.
52 Horiuchi T, Mitoma H, Harashima S, et al. Transmembrane TNF-alpha: structure, function and interaction with anti-TNF agents. Rheumatology 2010;49:1215–1228.
53 Kadijani AA, Aghdaei HA, Sorrentino D, et al. Transmembrane TNF-α density, but not soluble TNF-α level, is associated with primary response to infliximab in inflammatory bowel disease. Clin Transl Gastroenterol 2017;8:e117.
54 Grell M, Douni E, Wajant H, et al. The transmembrane form of tumor necrosis factor is the prime activating ligand of the 80 kDa tumor necrosis factor receptor. Cell 1995;83:793–802.
55 Theilgaard-Mönch K, Jacobsen LC, Borup R, et al. The transcriptional program of terminal granulocytic differentiation. Blood 2005;105:1785–1796.
56 Siegmund D, Kums J, Ehrenschwender M, et al. Activation of TNFR2 sensitizes macrophages for TNFR1-mediated necroptosis. Cell Death Dis 2016;7:e2375.
57 Maney NJ, Reynolds G, Krippner-Heidenreich A, et al. Dendritic cell maturation and survival are differentially regulated by TNFR1 and TNFR2. J Immunol 2014;193:4914–4923.
58 Defer N, Azroyan A, Pecker F, et al. TNFR1 and TNFR2 signaling interplay in cardiac myocytes. J Biol Chem 2007;282:35564–35573.
59 Naudé PJW, Den Boer JA, Luiten PGM, et al. Tumor necrosis factor receptor cross-talk. FEBS J 2011;278:888–898.
60 Wicovsky A, Henkler F, Salzmann S, et al. Tumor necrosis factor receptor-associated factor-1 enhances proinflammatory TNF receptor-2 signaling and modifies TNFR1–TNFR2 cooperation. Oncogene 2009;28:1769–1781.
61 Boström J, Sramkova Z, Salašová A, et al. Comparative cell cycle transcriptomics reveals synchronization of developmental transcription factor networks in cancer cells.

PLoS One 2017;12:e0188772.
62 Liu Y, Chen S, Wang S, et al. Transcriptional landscape of the human cell cycle. Proc Natl Acad Sci 2017;114:3473–3478.
63 Peña-Diaz J, Hegre SA, Anderssen E, et al. Transcription profiling during the cell cycle shows that a subset of Polycomb-targeted genes is upregulated during DNA replication. Nucleic Acids Res 2013;41:2846–2856.
64 Liu Z, Lou H, Xie K, et al. Reconstructing cell cycle pseudo time-series via single-cell transcriptome data. Nat Commun 2017;8:22.
65 Takashima A, Yao Y. Neutrophil plasticity: acquisition of phenotype and functionality of antigen-presenting cell. J Leukoc Biol 2015;98:489–496.
66 Nishikawa Y, Sone M, Nagahama Y, et al. Tumor necrosis factor-α promotes bile ductular transdifferentiation of mature rat hepatocytes in vitro. J Cell Biochem 2013;114:831–843.
67 Li B, Pozzi A, Young PP. TNF accelerates monocyte to endothelial transdifferentiation in tumors by the induction of integrin 5 expression and sdhesion to fibronectin. Mol Cancer Res 2011;9:702–711.
68 Bachem MG, Sell KM, Melchior R, et al. Tumor necrosis factor alpha (TNF alpha) and transforming growth factor beta 1 (TGF beta 1) stimulate fibronectin synthesis and the transdifferentiation of fat-storing cells in the rat liver into myofibroblasts. Virchows Arch B Cell Pathol Incl Mol Pathol 1993;63:123–130.
69 Lu X, Lu J, Liao B, et al. Driver pattern identification over the gene co-expression of drug response in ovarian cancer by integrating high throughput genomics data. Sci Rep 2017;7:16188.
70 Liu Z, Meng J, Li X, et al. Identification of hub genes and key pathways associated with two subtypes of diffuse large B-cell lymphoma based on gene expression profiling via integrated bioinformatics. Biomed Res Int 2018;2018:1–14.
71 Dolgin E. The greatest hits of the human genome: A tour through the most studied genes in biology reveals some surprises. Nature 2017;551:427–431.
72 Rowat AC, Jaalouk DE, Zwerger M, et al. Nuclear envelope composition determines the ability of neutrophil-type cells to passage through micron-scale constrictions. J Biol Chem 2013;288:8610–8618.
73 Jacobson EC, Grand RS, Perry JK, et al. Hi-C detects novel structural variants in HL-60 and HL-60/S4 cell lines. BioRxiv 2018:482208.
74 Harrow J, Frankish A, Gonzalez JM, et al. GENCODE: The reference human genome annotation for The ENCODE Project. Genome Res 2012;22:1760–1774.
75 Ewels P, Magnusson M, Lundin S, et al. MultiQC: Summarize analysis results for multiple tools and samples in a single report. Bioinformatics 2016;32:3047–3048.
76 Yu G, Wang L-G, Han Y, et al. clusterProfiler: an R package for comparing biological themes among gene clusters. Omi A J Integr Biol 2012;16:284–287.
77 Swinton J. Vennerable: Venn and Euler area-proportional diagrams.
78 Wikham H, François R, Henry L, et al. dplyr: A Grammar of Data Manipulation 2018.
79 Wikham H. ggplot2: Elegant Graphics for Data Analysis. Springer-Verlag New York, 2016.
80 Olarerin-George AO, Hogenesch JB. Assessing the prevalence of mycoplasma contamination in cell culture via a survey of NCBI's RNA-seq archive. Nucleic Acids Res 2015;43:2535–2542.
81 Schmittgen TD, Livak KJ. Analyzing real-time PCR data by the comparative C(T) method. Nat Protoc 2008;3:1101–1108.

Figure legends

Figure 1. Transcriptional changes in promyelocytic and granulocytic forms of HL-60/S4 following two hours of TNF-α treatment. A) The Log2 fold change (log2FC) and adjusted p values of all analyzed genes in promyelocytes with and without TNF-α treatment. B) The log2FC and adjusted p values of all analyzed genes in granulocytes with and without TNF-α treatment. C) There is a shared and unique transcriptional response to TNF-α treatment of HL-60/S4 promyelocytes and granulocytes. D) The log2FC of genes that were significantly differentially expressed in both HL-60/S4 and HL-60/S4+ATRA cells were positively correlated (R2=0.65). However, there was a small subset of genes that were anticorrelated. E) The log2FC of genes that were only differentially expressed in HL-60/S4 cells did not correlate between HL-60/S4 and HL-60/S4+ATRA after TNF-α treatment (R2=0.04). E) The log2FC of genes that were only differentially expressed in HL-60/S4+ATRA cells did not correlate between HL-60/S4 and HL-60/S4+ATRA after TNF-α treatment (R2=0.15).

Figure 2. Transcriptional changes in promyelocytes and granulocytes treated with TNF. Gene set enrichment analysis (GSEA) of genes represented in the MSigDB Hallmark gene sets [1]. All represented genes were ranked by Log2FC, with no significance cutoff. The x axis shows significantly enriched gene sets (FDR<0.05). The normalized enrichment score (y axis) indicates whether a given gene set was overrepresented for transcripts that exhibited large fold changes. Predicted gene sets (e.g. TNFA signaling via NFKB, p53 pathway, and IFNγ response) were enriched in both conditions. No gene sets were enriched in HL-60/S4 but not HL-60/S4+ATRA. Six gene sets (adipogenesis, estrogen response early and late, hypoxia, IFNα response, and xenobiotic metabolism) were enriched in HL-60/S4+ATRA, but not HL-60/S4.

Figure 3. Gene set overrepresentation in differential expression subsets of TNF-α treated promyelocytes and granulocytes. A) Genes that were significantly differentially expressed in the same direction after TNF-α treatment were overrepresented in several gene sets canonically associated with TNF-α response. B) Genes that were only significantly differentially expressed in granulocytes were overrepresented in 9 gene sets, including 4 cell cycle associated gene sets. They were also overrepresented in the reactive oxygen species pathway, a neutrophilic response to TNF-α. C) Genes that were significantly differentially expressed in opposite directions were overrepresented in two cell-cycle associated gene sets. All differentially expressed hallmark G2M checkpoint genes were upregulated in promyelocytes, and downregulated in granulocytes cells, with the exception of E2F2, a transcription factor that promotes quiescence by binding to promoters and transcriptionally repressing cell cycle genes [2]. All differentially expressed E2F2 target genes were upregulated in promyelocytes, and downregulated in granulocytes.

Figure 4. Transcriptional changes in promyelocytes differentiated into granulocytes with ATRA or macrophages with TPA, compared to TNF-α treatment of promyelocytes and granulocytes. Gene set enrichment analysis (GSEA) of genes represented in the MSigDB Hallmark gene sets [1]. All represented genes were ranked by Log2FC, with no significance cutoff. The x axis shows significantly enriched gene sets (FDR<0.05), and the y axis is calculated from the proportion of genes in the leading edge out of the number of ranked genes, and out of the gene set size. All conditions were associated with upregulated inflammatory gene sets, and both differentiation conditions were associated with downregulation of cell cycle gene sets.

Figure 5. Gene set overrepresentation in differential expression subsets of promyelocytes differentiated into granulocytes or macrophages. A) Genes that were significantly differentially expressed in the same direction after differentiation were overrepresented in gene sets associated with inflammatory signaling and cell cycle. B) Genes that were only significantly differentially expressed in cells differentiated into macrophages with TPA were predominantly associated with cell cycle. C) Genes that were significantly differentially expressed in opposite directions were overrepresented in 3 gene sets: IL2 STAT5 signaling, p53 pathway, and TNF-α signaling via NFKB. A majority of genes in all categories increased expression after macrophage differentiation and in granulocytes treated with TNF-α, and decrease expression after granulocytic differentiation. Non-significant changes are indicated with grey.

Table 1. Details of HL-60/S4 RNA-seq datasets. Four conditions in triplicate were generated in this study, while three conditions with four replicates were analysed from Welch et al. Cells were undifferentiated (promyelocyte), differentiated with ATRA (granulocyte) or TPA (macrophage). Promyelocytes and granulocytes in this study were treated with TNF or vehicle. The library preparation method in this study was ribosomal depletion to sequence all long RNAs, while Welch 2017 [30] used poly-A enrichment to sequence mRNA only. 'Reads sequenced' indicate the total number of paired-end reads generated per library. 'Reads mapped' indicate the number of read pairs aligned to the human genome with STAR [37]. 'Reads assigned' indicates the number of mapped reads assigned to genomic features (*e.g.* protein coding gene, non-coding RNA) with featureCounts [38].

Additional files

Additional file 1. Supplementary tables 1-22. 1. Significantly differentially expressed genes in promyelocytes treated with TNF-a, differentiated into granulocytes and macrophages, and granulocytes treated with TNF-a. 2. RT-qPCR and RNA-seq of *CDK1*, *TNF*, and *VCAM1*. 3-21. Functional analysis summary tables of GSEA, GO, KEGG, and hallmark terms enriched in subsets of differentially expressed genes. 22. Primers and probes used for RT-qPCR validation.

Additional file 2. Supplementary figure 1. PCA of VST-normalized transcript counts show conditions cluster together in A) promyelocytes treated with TNF-α, B) granulocytes treated with TNF-α, and C) promyelocytes differentiated into granulocytes and macrophages.

Competing interests

The authors declare that they have no competing interests

Funding
This research was supported by a Health Research Council Explorer grant (HRC 15/604) to JMO. ECJ and LJ were recipients of a University of Auckland doctoral scholarship, and ECJ of a Maurice Wilkins Centre travel grant. The funding bodies had no role in the study design, collection, analysis, and interpretation of the data or preparation of the manuscript.

Authors' Contributions

ECJ performed the experiments, analyzed and interpreted the data, and wrote the manuscript with support from JMO, JKP, and MHV. LJ performed and analyzed the RT-qPCR validation. All authors contributed to revisions and approved the final manuscript.

Acknowledgements
The authors would like to thank Peter Shepherd and the members of the JMO lab group for comments and discussion.

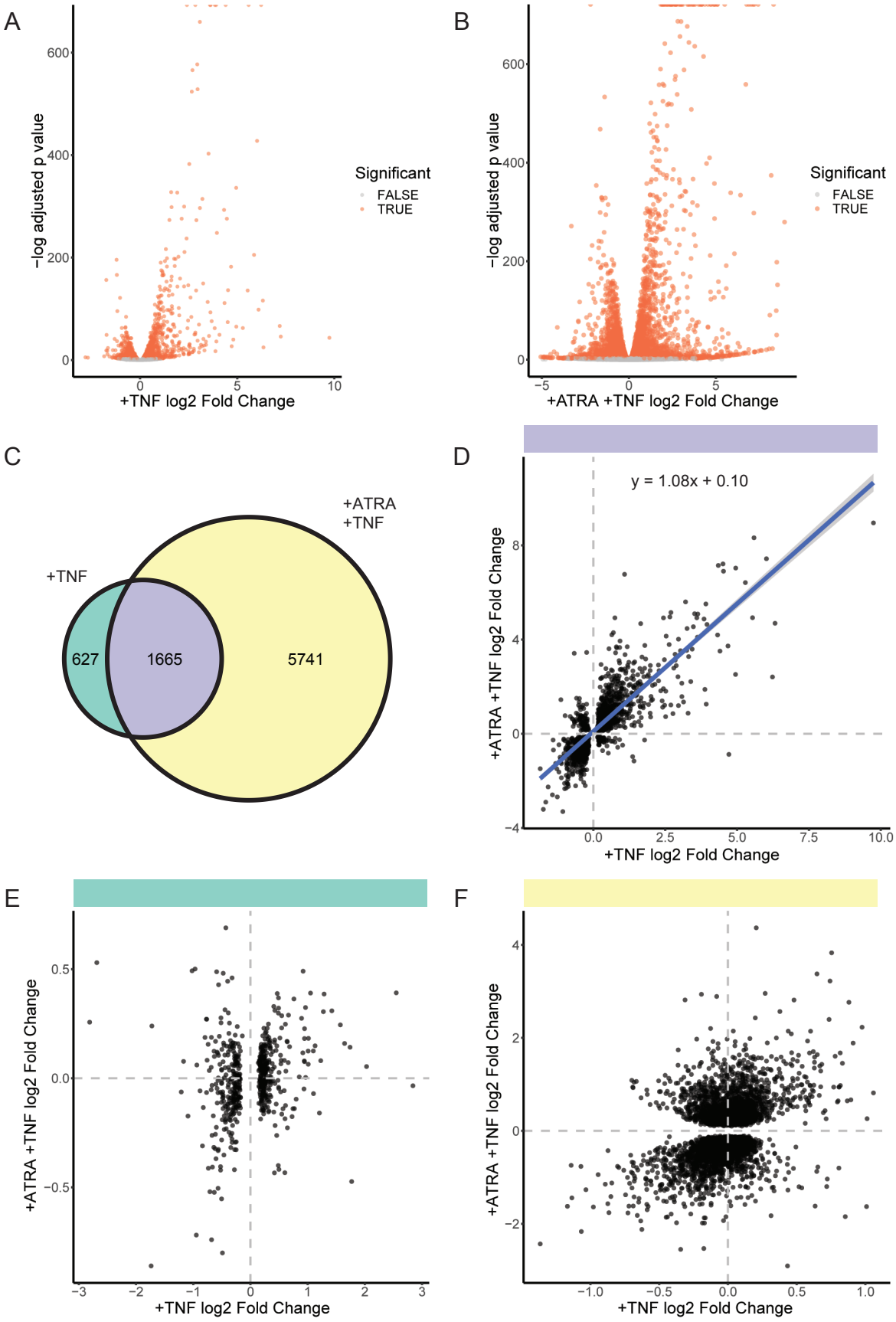
A
−log adjusted p value
+TNF log2 Fold Change
Significant
FALSE
TRUE
B
−log adjusted p value
+ATRA +TNF log2 Fold Change
Significant
FALSE
TRUE
C
+ATRA
+TNF
+TNF
627
1665
5741
D
y = 1.08x + 0.10
+ATRA +TNF log2 Fold Change
+TNF log2 Fold Change
E
+ATRA +TNF log2 Fold Change
+TNF log2 Fold Change
F
+ATRA +TNF log2 Fold Change
+TNF log2 Fold Change

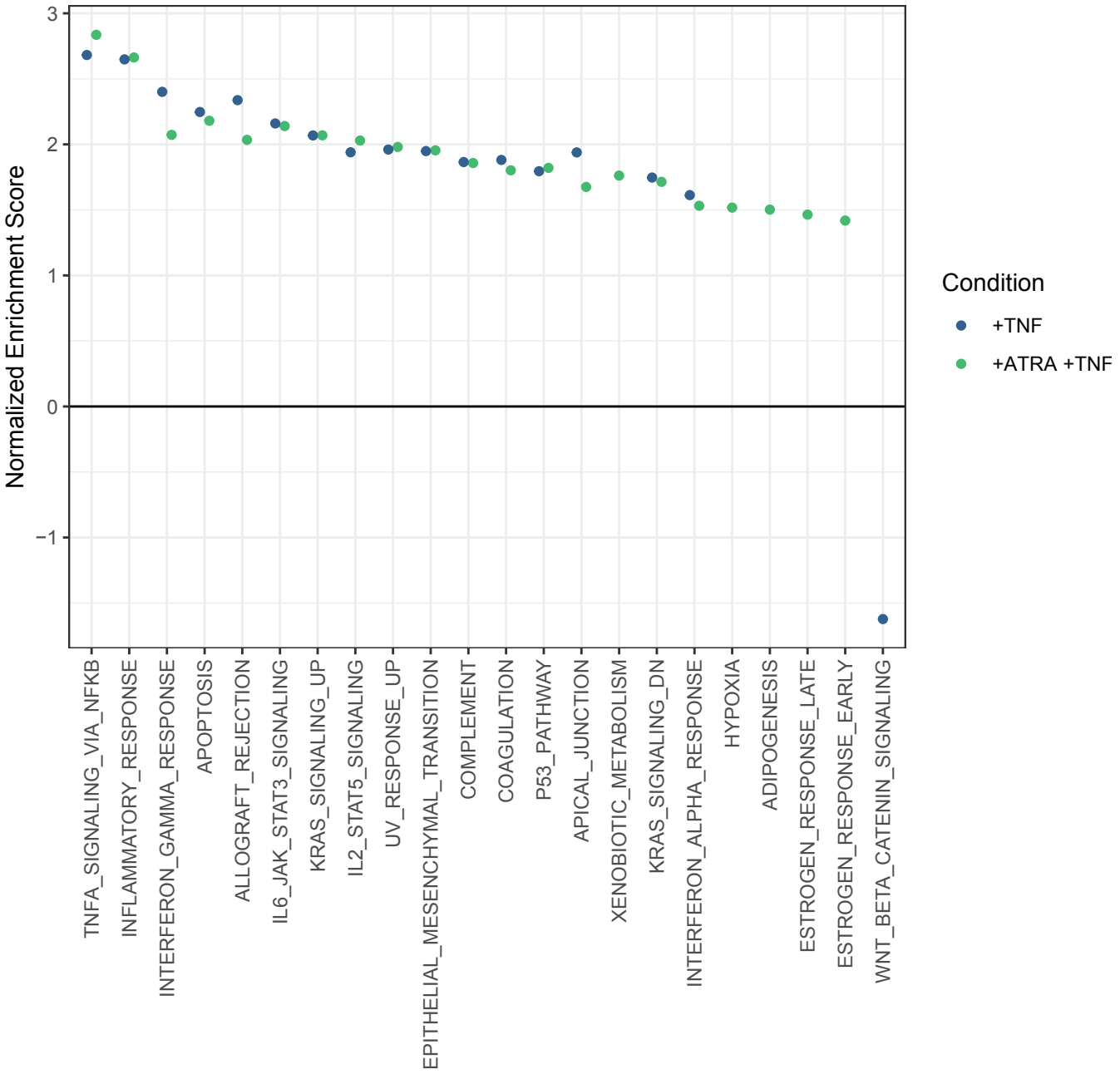
Normalized Enrichment Score
3
2
1
0
−1
TNFA_SIGNALING_VIA_NFKB
INFLAMMATORY_RESPONSE
INTERFERON_GAMMA_RESPONSE
APOPTOSIS
ALLOGRAFT_REJECTION
IL6_JAK_STAT3_SIGNALING
KRAS_SIGNALING_UP
IL2_STAT5_SIGNALING
UV_RESPONSE_UP
EPITHELIAL_MESENCHYMAL_TRANSITION
COMPLEMENT
COAGULATION
P53_PATHWAY
APICAL_JUNCTION
XENOBIOTIC_METABOLISM
KRAS_SIGNALING_DN
INTERFERON_ALPHA_RESPONSE
HYPOXIA
ADIPOGENESIS
ESTROGEN_RESPONSE_LATE
ESTROGEN_RESPONSE_EARLY
WNT_BETA_CATENIN_SIGNALING
Condition
+TNF
+ATRA +TNF

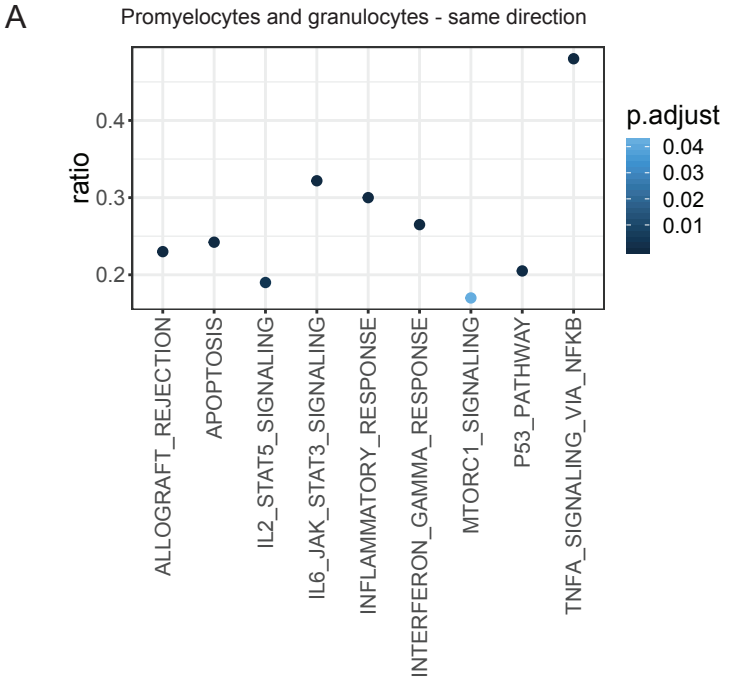
A
Promyelocytes and granulocytes - same direction
ratio
0.4
0.3
0.2
p.adjust
0.04
0.03
0.02
0.01
ALLOGRAFT_REJECTION
APOPTOSIS
IL2_STAT5_SIGNALING
IL6_JAK_STAT3_SIGNALING
INFLAMMATORY_RESPONSE
INTERFERON_GAMMA_RESPONSE
MTORC1_SIGNALING
P53_PATHWAY
TNFA_SIGNALING_VIA_NFKB

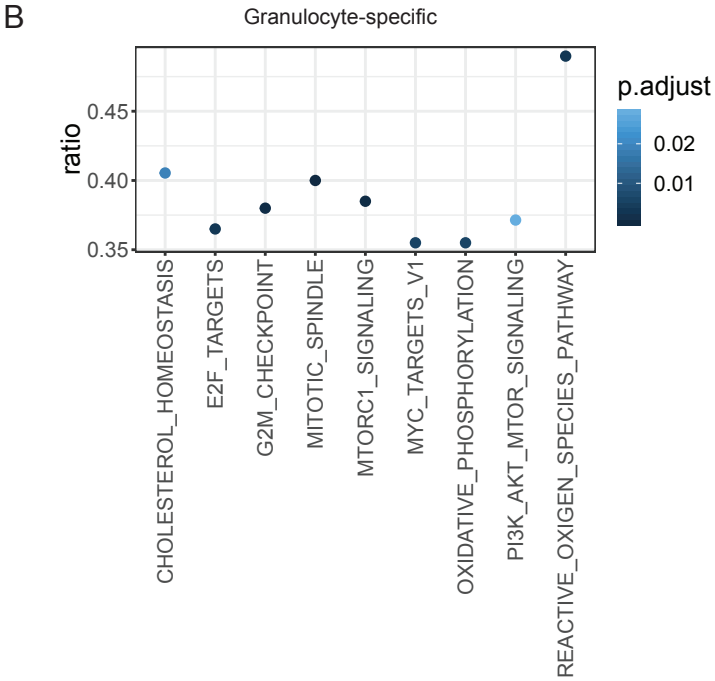
B
Granulocyte-specific
ratio
0.45
0.40
0.35
p.adjust
0.02
0.01
CHOLESTEROL_HOMEOSTASIS
E2F_TARGETS
G2M_CHECKPOINT
MITOTIC_SPINDLE
MTORC1_SIGNALING
MYC_TARGETS_V1
OXIDATIVE_PHOSPHORYLATION
PI3K_AKT_MTOR_SIGNALING
REACTIVE_OXIGEN_SPECIES_PATHWAY

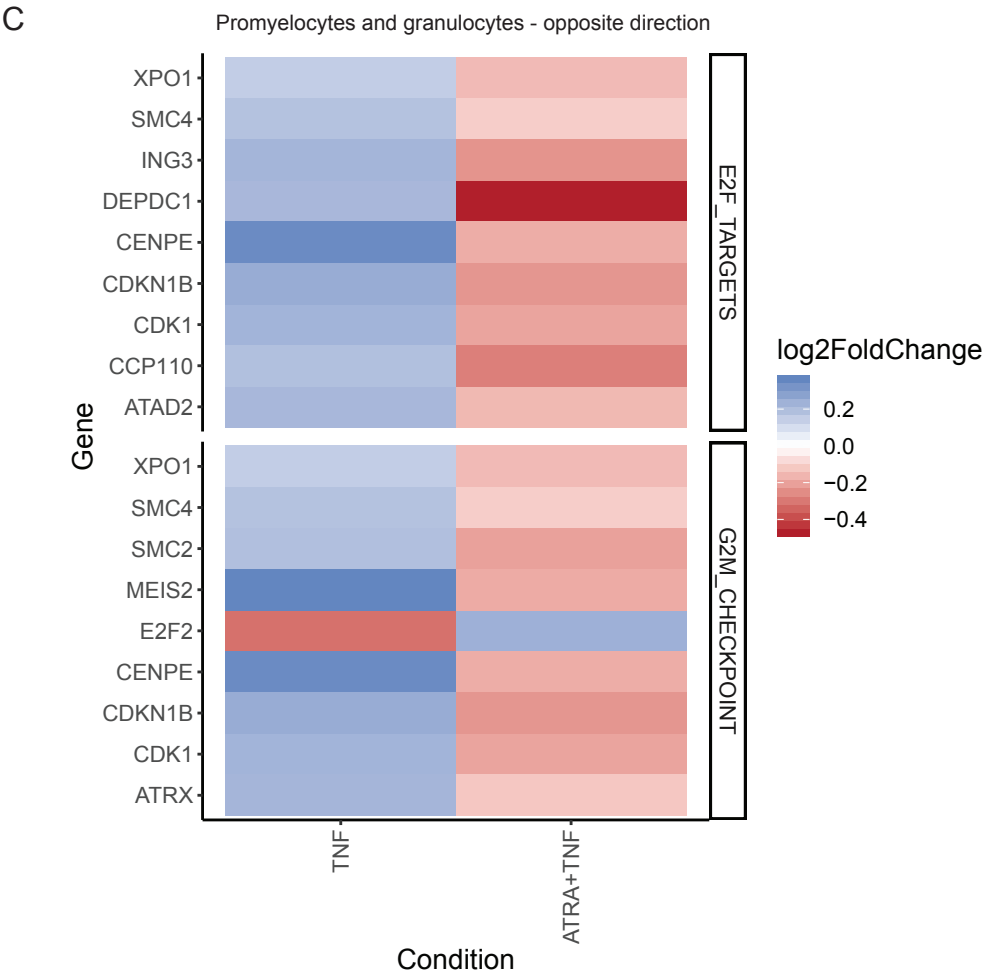
C
Promyelocytes and granulocytes - opposite direction
Gene
XPO1
SMC4
ING3
DEPDC1
CENPE
CDKN1B
CDK1
CCP110
ATAD2
E2F_TARGETS
XPO1
SMC4
SMC2
MEIS2
E2F2
CENPE
CDKN1B
CDK1
ATRX
G2M_CHECKPOINT
TNF
ATRA+TNF
Condition
log2FoldChange
0.2
0.0
−0.2
−0.4

Normalized Enrichment Score
2
0
−2
TNF
ATRA+TNF
ATRA
TPA
INFLAMMATORY_RESPONSE
TNFA_SIGNALING_VIA_NFKB
INTERFERON_GAMMA_RESPONSE
IL6_JAK_STAT3_SIGNALING
ALLOGRAFT_REJECTION
KRAS_SIGNALING_UP
IL2_STAT5_SIGNALING
INTERFERON_ALPHA_RESPONSE
UV_RESPONSE_UP
COMPLEMENT
APOPTOSIS
EPITHELIAL_MESENCHYMAL_TRANSITION
COAGULATION
TGF_BETA_SIGNALING
NOTCH_SIGNALING
MYOGENESIS
P53_PATHWAY
ANGIOGENESIS
APICAL_JUNCTION
XENOBIOTIC_METABOLISM
KRAS_SIGNALING_DN
HYPOXIA
UV_RESPONSE_DN
ESTROGEN_RESPONSE_EARLY
ANDROGEN_RESPONSE
CHOLESTEROL_HOMEOSTASIS
ADIPOGENESIS
ESTROGEN_RESPONSE_LATE
HEME_METABOLISM
DNA_REPAIR
OXIDATIVE_PHOSPHORYLATION
WNT_BETA_CATENIN_SIGNALING
SPERMATOGENESIS
G2M_CHECKPOINT
MYC_TARGETS_V2
MYC_TARGETS_V1
E2F_TARGETS
Condition
+TNF
+ATRA+TNF
+ATRA
+TPA

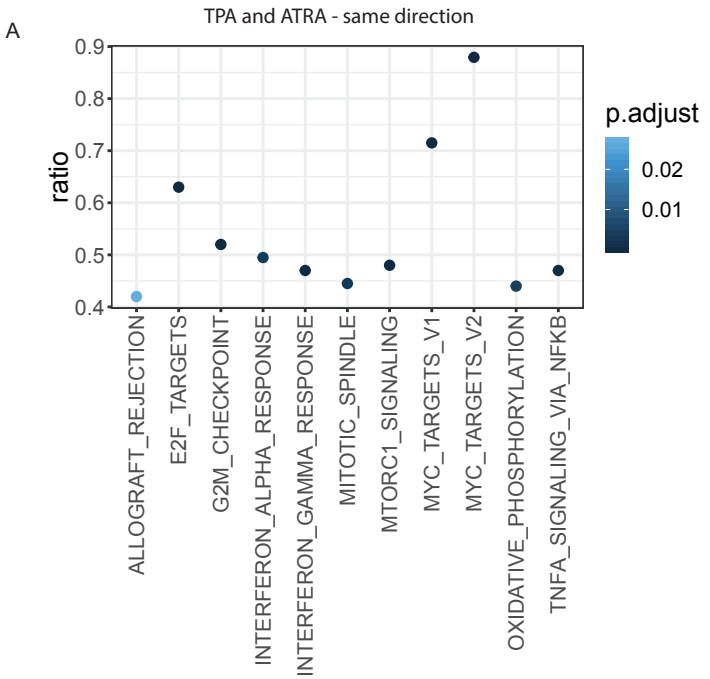
A
TPA and ATRA - same direction
ratio
0.9
0.8
0.7
0.6
0.5
0.4
ALLOGRAFT_REJECTION
E2F_TARGETS
G2M_CHECKPOINT
INTERFERON_ALPHA_RESPONSE
INTERFERON_GAMMA_RESPONSE
MITOTIC_SPINDLE
MTORC1_SIGNALING
MYC_TARGETS_V1
MYC_TARGETS_V2
OXIDATIVE_PHOSPHORYLATION
TNFA_SIGNALING_VIA_NFKB
p.adjust
0.02
0.01

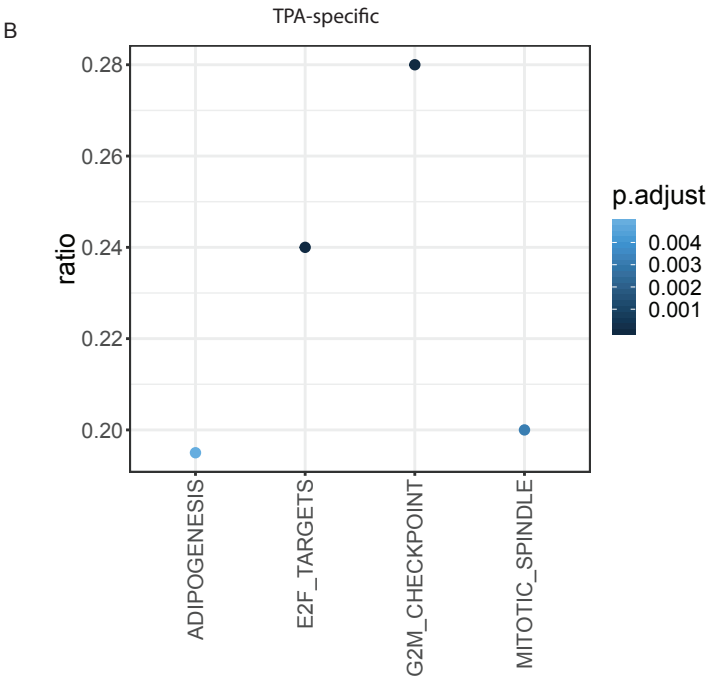
B
TPA-specific
ratio
0.28
0.26
0.24
0.22
0.20
ADIPOGENESIS
E2F_TARGETS
G2M_CHECKPOINT
MITOTIC_SPINDLE
p.adjust
0.004
0.003
0.002
0.001

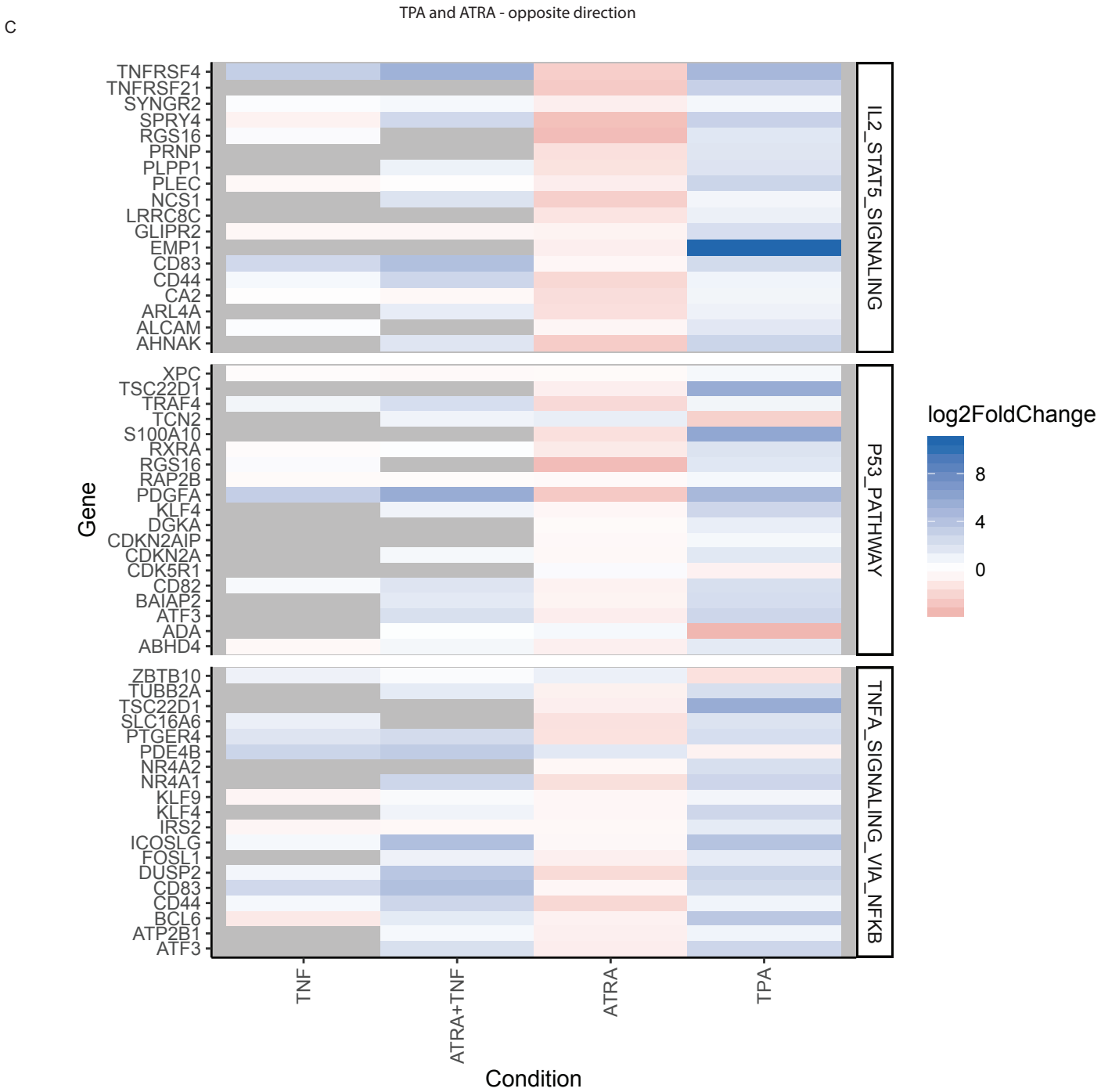
C
TPA and ATRA - opposite direction
Gene
TNFRSF4
TNFRSF21
SYNGR2
SPRY4
RGS16
PRNP
PLPP1
PLEC
NCS1
LRRC8C
GLIPR2
EMP1
CD83
CD44
CA2
ARL4A
ALCAM
AHNAK
IL2_STAT5_SIGNALING
XPC
TSC22D1
TRAF4
TCN2
S100A10
RXRA
RGS16
RAP2B
PDGFA
KLF4
DGKA
CDKN2AIP
CDKN2A
CDK5R1
CD82
BAIAP2
ATF3
ADA
ABHD4
P53_PATHWAY
ZBTB10
TUBB2A
TSC22D1
SLC16A6
PTGER4
PDE4B
NR4A2
NR4A1
KLF9
KLF4
IRS2
ICOSLG
FOSL1
DUSP2
CD83
CD44
BCL6
ATP2B1
ATF3
TNFA_SIGNALING_VIA_NFKB
TNF
ATRA+TNF
ATRA
TPA
Condition
log2FoldChange
8
4
0

Data source	Library type	Differentiation agent	Cell type	Treatment	Replicate	Reads sequenced	Reads mapped	Reads assigned
New data	Total	None	Promyelocyte	None	1	51,259,672	48,256,979	31,775,702
					2	45,409,486	43,088,708	26,931,181
					3	47,722,497	45,321,199	28,412,920
New data	Total	None	Promyelocyte	TNF	1	45,401,741	42,548,543	26,121,834
					2	46,622,711	44,003,082	28,053,460
					3	52,842,736	50,124,478	31,895,061
New data	Total	ATRA	Granulocyte	None	1	46,965,601	44,427,313	24,592,785
					2	53,329,425	50,564,062	28,655,822
					3	52,544,954	49,873,305	28,687,969
New data	Total	ATRA	Granulocyte	TNF	1	44,130,932	41,753,860	23,800,117
					2	55,591,032	52,524,970	29,318,607
					3	44,662,624	42,149,334	22,829,189
Welch 2017	mRNA	None	Promyelocyte	None	1	78,330,794	72,778,198	63,063,700
					2	79,840,457	74,010,895	63,896,640
					3	92,276,843	85,870,266	77,717,651
					4	71,908,445	67,034,452	61,274,376
Welch 2017	mRNA	ATRA	Granulocyte	None	1	78,215,359	73,037,649	63,738,330
					2	79,385,831	73,007,606	65,788,452
					3	67,293,855	61,810,327	55,209,128
					4	74,792,543	68,660,444	61,293,657
Welch 2017	mRNA	TPA	Macrophage	None	1	78,936,655	72,842,622	63,297,008
					2	75,555,764	69,802,997	59,853,678
					3	75,679,506	69,532,640	63,186,748
					4	70,096,915	65,311,735	59,900,363

Table 1. Details of HL-60/S4 RNA-seq datasets. Four conditions in triplicate were generated in this study, while three conditions with four replicates were analysed from Welch *et al*. 2017 [1]. Promyelocytes and granulocytes in this study were treated with TNF or vehicle. Cell treatment groups from Welch *et al.* were the following: undifferentiated (promyelocyte), differentiated with ATRA (granulocyte) or TPA (macrophage). The library preparation method in this study was ribosomal depletion to sequence all long RNAs, while Welch *et. al.* 2017 used poly-A enrichment to sequence mRNA only. 'Reads sequenced' indicate the total number of paired-end reads generated per library. 'Reads mapped' indicate the number of read pairs aligned to the human genome with STAR [2]. 'Reads assigned' indicates the number of mapped reads assigned to genomic features (*e.g*. protein coding gene, non-coding RNA) with featureCounts [3].

1 Mark Welch DB, Jauch A, Langowski J, et al. Transcriptomes reflect the phenotypes of undifferentiated, granulocyte and macrophage forms of HL-60/S4 cells. Nucleus 2017;8:222–237.
2 Dobin A, Davis CA, Schlesinger F, et al. STAR: ultrafast universal RNA-seq aligner. Bioinformatics 2013;29:15–21.
3 Liao Y, Smyth GK, Shi W. featureCounts: an efficient general purpose program for assigning sequence reads to genomic features. Bioinformatics 2014;30:923–930.